Journal of Coastal Research	18	4	622–636	West Palm Beach, Florida	Fall 2002

Waves and Currents During a Winter Cold Front in the Mississippi Bight, Gulf of Mexico: Implications for Barrier Island Erosion

Timothy R. Keen

Naval Research Laboratory
Oceanography Division
Stennis Space Center
MS 39529, U.S.A.
keen@nrlssc.navy.mil

ABSTRACT

KEEN, T.R., 2002. Waves and currents during a winter cold front in the Mississippi Bight, Gulf of Mexico: Implications for barrier island erosion. *Journal of Coastal Research*, 18(4), 622–636. West Palm Beach (Florida), ISSN 0749-0208.

This study uses numerical models to predict waves and currents in the Mississippi bight, Gulf of Mexico, for the period 4 to 7 March 1997, during which time a cold front passed over the region. The models are validated using observations from the area. The simulated waves and currents are used to infer littoral transport paths along the soundside of the barrier islands fronting Mississippi Sound and Chandeleur Sound. Predicted waves along the soundside of the barriers reach heights of 0.9 m with wave periods less than 4 s. These steep waves are important for eroding the soundside of the barrier islands. Currents near the barrier islands within Mississippi Sound are dominated by tidal flow. Consequently, shoreface transport within this estuary is sensitive to the tidal stage as well as wind direction and strength. Wave-driven littoral transport cells within Mississippi Sound are inferred to have been eastward during the frontal passage phase and westward as the wind became northeasterly during the post-frontal phase. This result suggests that sediment eroded from the barrier islands was continuously transported into tidal inlets. The model results also suggest that a southward wave-driven longshore drift cell was established along the soundside margin of the Chandeleur Island chain, with spillover onto the Gulf side of the southern islands.

ADDITIONAL INDEX WORDS: *Coastal erosion, cold fronts, barrier islands, numerical models, Mississippi bight, Gulf of Mexico.*

INTRODUCTION

The short-term exchange of sediment between the subaerial beach, shoreface, and inner continental shelf has a significant impact on commercial and residential construction, recreation, and military operations in the coastal zone. Consequently, among the tasks facing coastal planners today are understanding, predicting, and limiting beach and nearshore erosion during storms and meteorological fronts. One reason for increased concern is the expectation of greater storminess and rising sea level associated with global warming (JONES, 1994; HAYDEN, 1999). Greater use of the coastal zone has also led to an increase in public awareness of coastal erosion problems. Damage to commercial and residential property by tropical and extratropical cyclones has reinforced the severity of the problem (STONE *et al.*, 1997; ZHANG *et al.*, 2000). Furthermore, the U. S. Navy has shifted its focus to littoral warfare and thus to nearshore hydrodynamics and the morphologic response of the beach-shoreface system (HARDING *et al.*, 1999). The increased interest in understanding coastal erosion makes it necessary to develop a more general capability for predicting nearshore sediment transport and morphology. This paper addresses this issue by discussing the use of several oceanographic forecasting tools to predict coastal erosion during a winter cold front in a low energy environment. This is an important development because of the need to make the maximum use of available environmental information in coastal studies.

00140 received 17 October 2000; accepted in revision 10 April 2002.

Background

The most costly damage to the U. S. Atlantic and Gulf of Mexico coastline is incurred when hurricanes and tropical storms make landfall (STONE *et al.*, 1997; PIELKE and LANDSEA, 1998). This economic problem was dramatized when Hurricanes Opal and Erin struck the Florida Gulf coast in 1995, which was one of the most intensive hurricane seasons in over 100 years of records (LAWRENCE *et al.*, 1998). The morphological impact of hurricanes can also be extreme in the Gulf of Mexico. For example, Hurricane Frederick flattened the Chandeleur Islands near the Mississippi River delta (KAHN and ROBERTS, 1982) and Hurricane Andrew caused permanent erosion and loss of wetlands along the Louisiana Gulf coast (STONE and FINKL, 1995). Extratropical cyclones are more important at mid-latitudes because these "northeasters" are much larger and more common than tropical cyclones. Thus, they can have long-term impacts on a greater extent of coast (DOLAN *et al.*, 1988; FENSTER and DOLAN, 1994; YOUNG *et al.*, 1995).

The most common meteorological events in coastal areas

are cold fronts, which occur with a frequency on the order of 1 week. The relationships between nearshore waves and currents, sediment concentrations, and erosion/deposition patterns during frontal passage have been examined by a number of authors (DAVIS and FOX, 1975; DINGLER *et al.*, 1993; CHANEY and STONE, 1996; ADDAD and MARTINS-NETO, 2000; PEREZ *et al.*, 2000). Although the waves and currents during cold fronts are weaker than during extratropical and tropical cyclones, they occur more frequently and can be as important for the evolution of low energy coasts in the Gulf of Mexico (ROBERTS *et. al.*, 1987; MOELLER *et al.*, 1993; HUH *et al.*, 2001). For example, rapid erosion of soundside beaches of barrier islands threatens a national historical monument in Mississippi Sound (Figure 1), prompting the National Park Service (NPS) to initiate a measurement program in order to develop a preservation plan (STONE *et al.*, 1998).

Understanding coastal change has been aided by the development of a range of predictive geomorphic models. Predictions of nearshore topography and coastal change can be made using process-response models, which are not easily applied to new areas because they use parameterizations for physical processes that may be site dependent (BRUUN, 1954; WRIGHT and SHORT, 1984; STONE and STAPOR, 1996). Mathematical models can be used to predict nearshore sedimentation during time intervals with more limited measurements but they still rely on local parameterizations (FOX and DAVIS, 1973; HANSON and KRAUS, 1989). Comprehensive numerical models substitute measurements for parameterizations of forcing fields to directly calculate nearshore sediment transport fluxes (BOWEN, 1980; BAILLARD, 1982; DALLY and DEAN, 1984; THIELER *et al.*, 2000) and they have proven useful in understanding erosion and depositional cycles if observations are available to drive them.

Local, state, and federal agencies are responsible for operating coastal current and wave forecast models on a semi-continuous basis in several areas within the United States, including the east coast (AIKMAN *et al.*, 1996), the west coast (CLANCY *et al.*, 1996), and the Great Lakes (SCHWAB and BEDFORD, 1994), as well as Tampa Bay (VINCENT *et al.*, 2000) and Galveston Bay (SCHMALZ, 2000) in the Gulf of Mexico. The U.S. Navy also has operational wave and current models running in different regions of the world (HORTON *et al.*, 1992). The increasing use of numerical wave and current models for both civilian and military coastal ocean forecasting suggests that now is the time to begin examining methods of coupling this growing coastal forecasting capability to coastal geomorphology models. One possible approach uses either model predictions or observations of the coastal wind, currents, and waves to drive morphodynamic or sedimentation models (KEEN and SLINGERLAND, 1993; KIM *et al.*, 1998; LEHFELDT and BARTHEL, 2000). Within this context, this paper will demonstrate that numerical wave and current models now have the required spatial and temporal resolution to supply forcing fields to geomorphic models and thereby permit improvements in studying coastal change at a range of scales.

Objectives

The overall objective of this paper is to demonstrate the usefulness of the simulated wave and current fields from numerical models in predicting event-driven changes in coastal morphology. This objective is accomplished by examining model simulations of currents and waves during a cold front that passed over the Mississippi bight (Figure 1) in March 1997. First, observations are used to characterize the physical forcing during the cold front. Then, the simulated waves and currents are compared to available measurements in order to evaluate the accuracy of the numerical models. The subsequent discussion of the predicted waves and currents will permit a qualitative analysis of coastal erosion in this region. Finally, the importance of having high-resolution, spatially and temporally variable waves and currents for predicting localized coastal erosion will be shown using example locations from within the Mississippi bight during the cold front.

STUDY AREA

The Mississippi bight (Figure 1) contains two large sounds fronted by barrier island chains, Mississippi Sound on the north and Chandeleur Sound on the west. The south-facing barrier islands that border Mississippi Sound were formed by upward aggradation as sediment from Mobile Bay was transported westward by longshore currents (OTVOS, 1970; 1979). Sediments within Mississippi Sound consist of medium to coarse sand along the barrier islands and silt and clay located within the central parts (UPSHAW *et al.*, 1966). Overall, the east-west lying barrier islands are migrating westward in response to wave-driven longshore drift (RUCKER and SNOWDEN, 1990; CIPRIANI and STONE, 2001). Ship Island has been repeatedly breached, most recently by Hurricane Camille in 1969, and today it comprises West Ship Island (WSI) and East Ship Island (ESI). West Ship Island has recently slowed its migration because of dredging in the ship channel to the west.

The Chandeleur Islands are a curved, east-facing barrier chain fronting Chandeleur Sound. These islands have continually migrated west-northwest over the subsiding St. Bernard deltaic plain (SUTER *et al.*, 1988). Beach deposits consist of shell fragments and fine quartz sand whereas the sediments of Chandeleur Sound comprise clay, silt and sand (KAHN and ROBERTS, 1982). The dominant geomorphic factors in the evolution of the Chandeleur barrier island chain are tropical cyclones, which commonly overwash and incise channels in these low-lying islands. The beaches of the southern islands are more exposed to storm waves than the northeast-facing beaches of the northern islands, which are shielded from the largest waves. The southern islands are therefore undergoing more rapid erosion and northwest migration than the northern islands. The established dunes of the northern islands also contribute to their durability by directing storm overwash into pre-existing channels. KAHN and ROBERTS (1982) noted that fairweather waves and currents rapidly redistributed sediment eroded from the beach and dune system by Hurricane Frederick, 1979. Much of this transported sediment contributes to the longshore drift pool that can rapidly seal storm channels (NUMMEDAL *et al.*, 1980). Hurricane Frederick flattened the southern Chandeleur Islands and they re-

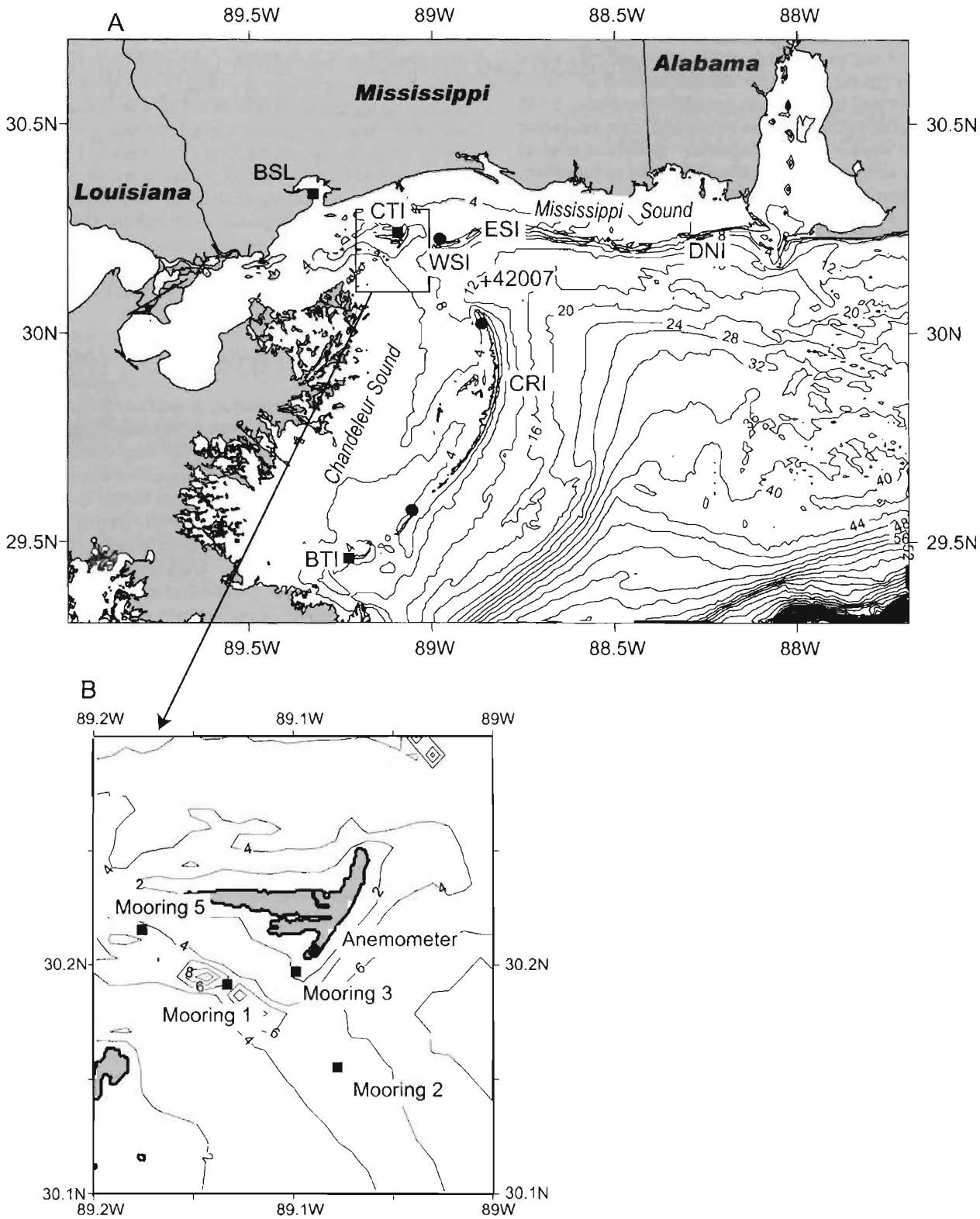

Figure 1. (A) Map of the Mississippi bight study area. The barrier islands are denoted as follows: DNI, Dauphin Island; ESI, East Ship Island; WSI, West Ship Island; CTI, Cat Island; CRI, Chandeleur Islands. The other symbols are: BSL, Bay St. Louis; 42007 (+), NOAA buoy 42007; BTI, Breton Isle. The squares indicate tidal stations used for model comparison. The circles are locations where model-predicted waves are discussed in text. (B) Inset map of the Cat Island observation program area. The moorings are listed in Table 1. Bathymetry is in meters.

Table 1. *Measured hydrographic timeseries at Cat Island, March 4-6, 1996.*

	Mooring 1	Mooring 2	Mooring 3	Mooring 5
Location	30.19220°N 89.14355°W	30.16730°N 89.09635°W	30.19532°N 89.12553°W	30.21270°N 89.12867°W
Depth	12.9 m	7.1 m	2.5 m	6.8 m
Surface	currents, temperature, salinity	currents, temperature, salinity	currents, temperature, salinity	currents, temperature, salinity
Bottom	NA	pressure temperature salinity transmissometer	temperature	temperature

main a shoal today because of more recent storms such as Hurricane Georges, 1998 (STONE and WANG, 1999).

Previous work in the Mississippi bight suggests that wave transport is not significant (KNOWLES and ROSATI, 1988); however, that study focused on steady state waves propagating from offshore. In order to assess the potential of wave-driven erosion within semi-enclosed bays and sounds it is necessary to measure the wave climate inside estuaries and use a time-dependent wave model that can capture the complex wave field during cold fronts. Furthermore, understanding sediment transport on the shoreface within the sounds makes it necessary to examine tidal and wind-driven currents inside the barrier islands. Work of this type is being undertaken by a joint effort of the Naval Oceanographic Office and the Environmental Protection Agency (BLUMBERG *et al*, 2000; AHSAN *et al.*, 2001).

METHODS

Field Measurements

After examining the Fleet Numerical Meteorological and Oceanographic Center forecasts and the local weather reports, an array of instruments (Table 1) was deployed on March 4, 1997 in anticipation of frontal passage. A cold front passed over the area on March 6 and the instruments were retrieved on March 7. The instruments were located to examine the sensitivity of inlet flow to the variable winds during a cold front and to validate numerical wave and current models for use in enclosed coastal waters like Mississippi Sound.

Timeseries of the wind speed and direction were measured at buoy 42007, operated by the National Oceanic and Atmospheric Administration (NOAA). This buoy is located in a water depth of 15 m near the northern end of the Chandeleur Islands (see Figure 1 for location). A second anemometer was placed on the southern end of Cat Island to evaluate differences in the wind over water and the low-lying islands. The significant wave height and period were measured at buoy 42007 and at mooring 2, located south of Cat Island. Water levels were also measured at mooring 2 using a bottom-mounted pressure gauge. Several CTD profiles were measured on March 4 and again on March 7.

Numerical Modeling of Waves and Currents

In order to examine the physical processes that affect barrier island erosion within the Mississippi bight during cold fronts, it is convenient to use numerical wave and current models. It is not sufficient to calculate the steady currents due to the tides and wind only because beach erosion is dominated by waves, even inside the barrier islands. Consequently, this study utilizes the third-generation spectral SWAN model (Simulating Waves Nearshore) (BOOIJ *et al.*, 1999; RIS *et al.*, 1999) to compute waves. The SWAN model is designed for application to shallow water regions. Input consists of bathymetry, water level changes, and wind fields. The model can also accept deepwater wave forcing at the open boundary. It calculates refraction, wave breaking, dissipation, wave-wave interaction, and local wind generation. The model does not compute diffraction and it should not be used when wave heights are expected to vary over a few wavelengths. Thus, the wave field is not generally accurate within the immediate vicinity of obstacles. It has been shown to produce reasonable results within the Mississippi bight (HSU *et al.*, 2000; ROGERS *et al.*, 2001). Dissipation of wave energy is computed for whitecapping, bottom friction, and depth-induced wave breaking. SWAN uses whitecapping formulations as adapted by the WAMDI Group (1988). The depth-induced dissipation formulation in the model is based on the JONSWAP bottom friction formulation with a friction coefficient of 0.067 m^2s^{-3} (HASSELMANN *et al.*, 1973).

The steady currents are calculated by the Princeton Ocean Model (hereinafter called POM) (see OEY and CHEN, 1992). The POM solves the primitive equations for momentum, as well as salinity, temperature, turbulent energy and a turbulent length scale (MELLOR and YAMADA, 1982). This model uses split modes; a small time step is used to solve for the depth-integrated flow (external or barotropic mode) and a larger time step is used to compute three-dimensional variables (internal or baroclinic mode). The model uses a terrain-following σ coordinate system in the vertical. The input to POM consists of bathymetry, initial three-dimensional salinity and temperature fields, heat and momentum fluxes at the surface, and the water surface anomalies, transports, and temperature and salinity values at open boundaries.

The wave and current models require both initial conditions and boundary forcing to operate. The atmospheric forcing for this study is supplied by the hourly winds measured at NOAA buoy 42007 (Figure 2). No heat fluxes are applied to the POM because of the uncertainty of these calculations in coastal areas, especially for short simulations. The initial temperature and salinity fields are derived from CTD profiles measured at mooring 2 on March 4. The Naval Oceanographic Office compiled the bottom topography from a variety of sources, including the National Ocean Service 3 second database. No open ocean boundary condition is used with SWAN because this study is focusing on processes within the

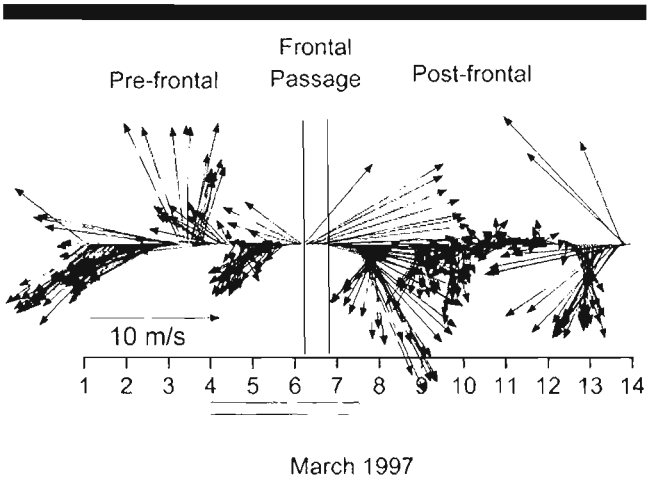

Figure 2. Vector plot of the wind time series measured at NOAA buoy 42007 for March 1–14, 1997. The horizontal bar indicates the interval during which the field measurements were made.

estuary, within which waves are generated by the local wind. The POM has an open boundary condition that includes the following: (1) tidal elevations and depth-integrated transports from the ADCIRC database for the East Coast and Gulf of Mexico (LEUTTICH *et al.*, 1992); (2) relaxation of salinity and temperature to the initial condition on inflow; and (3) a radiation condition for both baroclinic and barotropic waves generated within the model domain (FLATHER, 1976). No river inflow is used for these short simulations.

Three hydrodynamic simulations were used in this study. The first uses a barotropic model with tidal forcing using boundary condition (1). This model is used to examine the ability of the POM to capture the fundamental dynamics as represented by tidal flow. A second barotropic model is used to examine the wind-driven water levels within the region. This model uses only wind forcing and closed boundaries. It is useful for evaluating small water level changes within the estuary caused by the wind during the cold front. These water level changes are independent of the astronomical tides. The third model is a baroclinic POM using all three boundary conditions. It is a hindcast, which will be compared to the observations and used to examine steady currents in the area.

The hydrodynamic simulations were calculated on a Cartesian grid with a horizontal resolution of 777 m along the x axis and 898 m along the y axis. The Princeton model was run with 11 σ-levels. The external time step is 6 seconds and the internal time step is 180 seconds. The model was spun up for 48 hours with tidal forcing only. It was then run with tidal and wind forcing for March 4–7, 1997. The SWAN model was run on a grid with x and y cell sizes of 965 m and 1112 m, respectively. A time step of 6 minutes was used in order to capture the rapid wave growth during the frontal passage phase of the cold front.

RESULTS

This section discusses waves, currents, and water level anomalies that were measured within the Mississippi Bight during March 1997. Since these same variables are predicted by the numerical models, it is important to differentiate observations from predictions in the subsequent discussion. Therefore, the following convention will be used; measurements will be described and discussed in the past tense, and model predictions and other calculations (like wave steepness) will be presented using the present tense. This convention underscores the fact that the measurements are unique and cannot be reproduced whereas the computations can be redone.

Observations During a Cold Front

The measured wind speed and direction at buoy 42007 (Figure 2) indicate the passage of cold fronts on March 3, 6, and 13; this pattern is typical of winter cold fronts within this region. The present discussion is focusing on the cold front of March 6. Following ROBERTS *et al.* (1987), we define the pre-frontal phase as being dominated by southerly winds. The pre-frontal phase of the cold front of March 6 was abbreviated somewhat because of the short time interval since the previous cold front. Thus, the wind rotated clockwise from northeasterly (blowing from northeast to southwest) to southeasterly just before the front arrived on March 6. During the frontal passage phase, the wind rapidly changed direction from southerly to westerly and a maximum wind speed of 12 m s^{-1} was measured. The post-frontal phase, which is defined as the period during which the wind becomes northerly, began on March 7. The measured wind at Cat Island (not shown) was very similar to that at the buoy but it was slightly weaker and more variable.

All of the waves generated within the sounds are fetch-limited during cold fronts and depth-limited wave growth occurs over shoals and near islands. The observed waves at mooring 2 are very similar to the open Gulf mooring but their period is much shorter because of the shallower water. The measured significant wave heights H_s during the cold front were similar on the open shelf at buoy 42007 and inside Mississippi Sound at mooring 2. The observed H_s at buoy 42007 (Figure 3) was less than 0.5 m during the pre-frontal phase and the significant wave period T_s was 4 s. The corresponding deep-water wavelength, calculated from $L_0 = T_s^2 g/2\pi$ (where g is the gravitational acceleration, 9.81 m s^{-2}), is 25 m and the wave steepness H_s/L_0 is 0.02; a value of 0.025 is commonly used as the boundary between "steep" and "low" waves (FRIEDMAN and SANDERS, 1978). Steep waves can deliver more wave energy to the beach and thus cause greater erosion than low waves. The waves on the inner shelf were low even during frontal passage when the observed H_s at 42007 increased to 1 m. The measured H_s at mooring 2 was below 0.25 m prior to the front and T_s fluctuated between 2 and 4 s, corresponding to a wave steepness of 0.04 and 0.01, respectively. The strengthening wind on March 6 generated waves with significant wave heights greater than 1.5 m at mooring 2, but with no increase in period until late in the day. Consequently, the wave steepness reached 0.24 when the waves were largest on March 7. The estimated wave steepness decreases significantly thereafter as the period increased to 6 s. The measured H_s at mooring 2 increased to

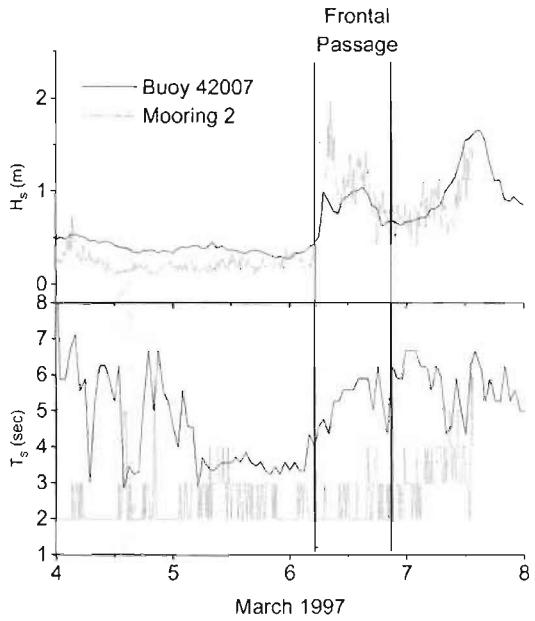

Figure 3. Time series plots of significant wave height (upper) and period (lower) measured at buoy 42007 and mooring 2.

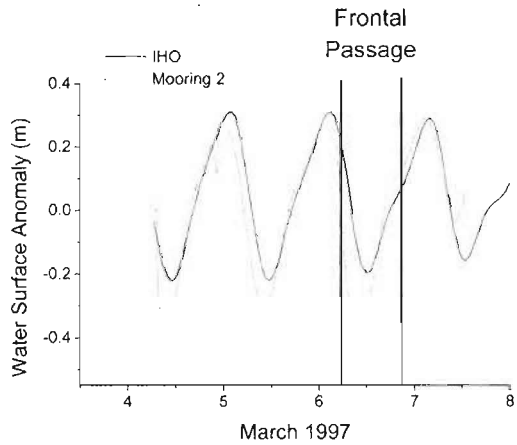

Figure 4. Time series plot of predicted water surface anomalies at Cat Island from the International Hydrographic Office (IHO) database, and the measured anomalies at mooring 2 from this study.

1.7 m in response to the strong northerly wind of March 7. The wind weakened significantly on March 8, however, and the measured H_s at buoy 42007 decreased rapidly.

The water level in Cat Island Channel is positively correlated with water levels within Mississippi Sound; *i.e.,* negative water surface anomalies (setdown) at mooring 2 (see Figure 1B for location) indicate a decrease in water level within the sound. The measured water level record at mooring 2 (Figure 4) indicates setdown relative to the tide predictions from the International Hydrographic Office (IHO) database for March 4–7. Northeasterly winds during the pre-frontal phase had pushed water out of Mississippi Sound and produced a maximum setdown near Cat Island at 1000 GMT on March 4. The water level at mooring 2 subsequently rose as the wind shifted to easterly immediately prior to frontal passage. However, the water surface anomaly became negative again during frontal passage when a westerly wind pushed water through the inlet north of the Chandeleur Islands; a maximum setdown of −0.25 m was measured at 1100 GMT on March 6. Northwesterly winds during the post-frontal phase were not aligned with this pass and flow was therefore reduced on March 7, producing a positive anomaly of 0.12 m at 1200 GMT. Water level anomalies within the rest of Mississippi Sound will be examined using the Princeton Ocean Model in a later section.

Tidal flow predominantly enters Mississippi Sound to the east and exits in the west through Ship Island Pass and Cat Island Channel; thus, the measured currents within Cat Island Channel were asymmetrical, with a northwest-southeast orientation along the channel axis. Measured peak velocities exceeded 1 m s^{-1} during the ebb tide at mooring 1 (Figure 5). The southeasterly wind between 0000 and 1200

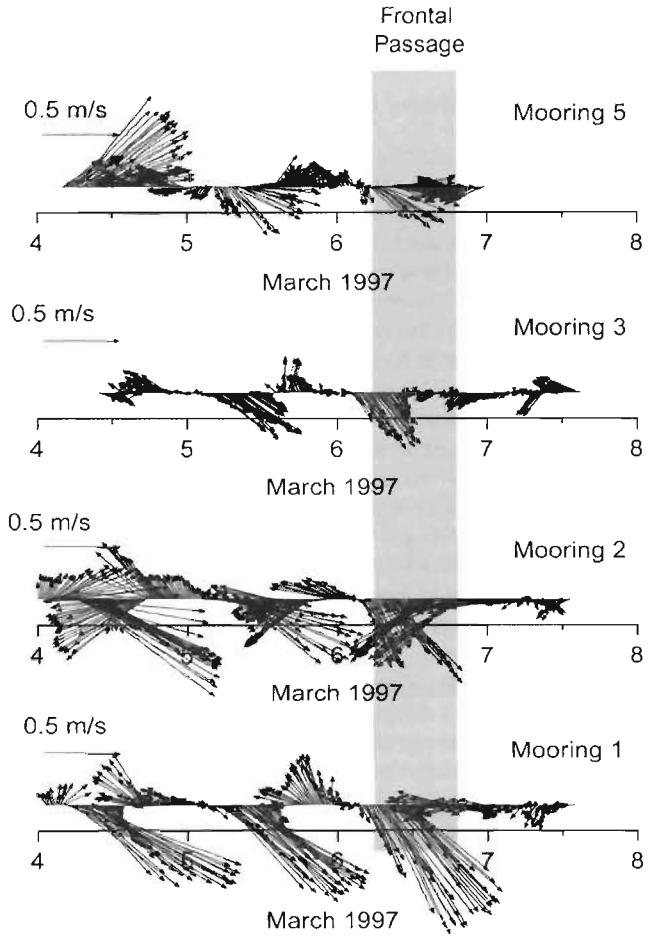

Figure 5. Vector plots of surface current time series measured in Cat Island Channel. See Figure 1 for locations.

GMT on March 4 drove a northward flow through the channel, as measured at moorings 1, 2, and 5. The measured currents at moorings 1, 3, and 5 were dominantly tidal during the easterly wind of March 5 because of the shadowing effect of Cat Island. Mooring 2 was located south of Cat Island Channel and, although the currents show a strong tidal signal, the flow was more responsive to the wind than at the other moorings. For example, northeasterly winds on March 5 generated southwestward currents at mooring 2 while flow remained to the southeast at the other moorings. The strong westerly winds on March 6 opposed the flood tide and the measured surface currents decreased at all of the moorings, with the exception of several southwest jets that were measured at mooring 2 near midday.

The observations indicate the complexity of flow within Mississippi Sound during a typical winter cold front. However, the measurements are inadequate to describe the wave and current fields throughout the Mississippi bight. The next section will describe numerical simulations of the waves and currents during the cold front and compare the model predictions to the available observations. This comparison will show that the models reproduce the measured waves, water surface anomalies, and currents within Mississippi Sound and adjacent coastal waters very well. The numerical model predictions can then be used with some confidence to examine the waves and currents throughout the estuary.

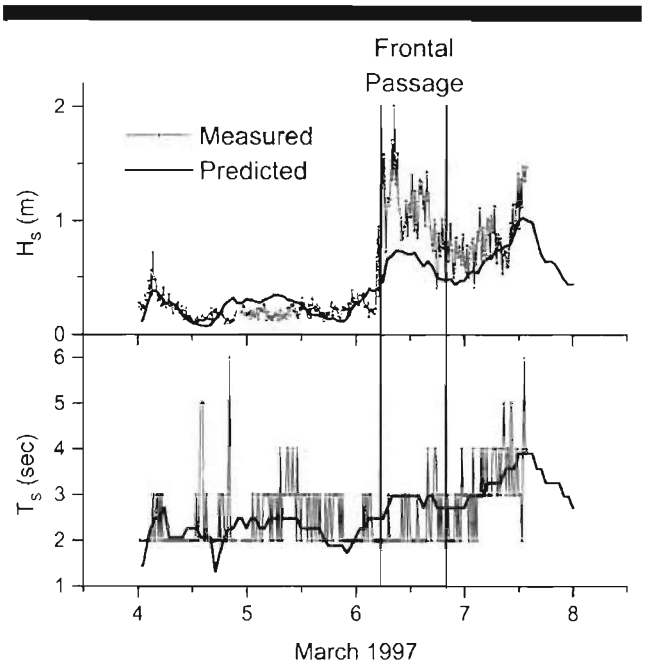

Figure 6. Significant wave height and period predicted by SWAN (thick solid line) and measured at mooring 2 (thin line with pluses).

Comparison of Model Predictions and Observations

The most important reason for using numerical hydrodynamic models like SWAN and POM is their incorporation of nonlinear physical processes such as bottom friction and advection. It is also useful that they have been used for a large number of applications and their general skill is reasonably well known. It is nevertheless important to validate their general behavior for individual studies, because of uncertainties in environmental forcing and bathymetry. This study focuses on waves and currents within the enclosed waters of the Mississippi bight. The comparison of modeled and measured waves and currents is thus restricted to observations made behind the barrier islands. The evaluation of the SWAN-predicted waves is limited to H_S and T_S. The measurements at mooring 2 are good for evaluating the wave model because it was located where the waves would be sensitive to fetch-limited growth as the wind changed direction. No other wave observations were available within the sound for the study interval. The model-predicted values of H_s (Figure 6) are accurate during the pre-frontal phase but the match deteriorates during frontal passage, when the maximum simulated waves are only 0.7 m. However, the model skill improves during the post-frontal phase. The large discrepancy during frontal passage may be due to wave generation by local winds within the sound because the wind field in the model was uniform. The values of T_S were predicted best during frontal passage, and were generally under-predicted during the pre-frontal and post-frontal phases. Nevertheless, the mean error for the model-predicted wave height is only 0.015 m, and for the predicted period it is 0.66 s. The standard deviations of the error for H_S and T_S are 0.19 m and 0.58 s, respectively. This good agreement between the model and the observations in a complex part of the bight indicates that the SWAN model will predict waves accurately elsewhere within the region. This assumption is supported by previous wave comparisons within the Mississippi bight (Hsu *et al.*, 2000; Rogers *et al.*, 2001).

In order to evaluate the predicted tidal elevations, the POM was run with tidal forcing only at the open boundary and no wind. The POM predictions of tidal water levels are compared to the IHO tidal elevations for March 4–14 at three locations within the estuary in Figure 7 (see Figure 1 for locations). The mean and standard deviation of the tidal elevation error at Cat Island are −0.033 m and 0.03 m, respectively, with the greatest error during the neap tide when the tidal range is less than 0.1 m. There is a slight phase error at Breton Isle and the resulting mean error is zero whereas the standard deviation of the error is 0.04 m. The amplitude error during the neap tide is greater at Bay St. Louis, because the model does not resolve the bay's complex shape. Nevertheless, the mean error is only 0.008 m and the standard deviation of the error is 0.053 m. The POM reproduces the tidal elevations well during the time of interest for this study at all three stations. This gives greater confidence for using it to evaluate steady flow in other parts of the tide-dominated estuary.

The POM can also be evaluated with respect to both calculated water levels and surface currents using the measurements from Cat Island Channel. For this comparison, the model is operated in three-dimensional baroclinic mode and forced with winds and tidal boundary conditions. The predicted water level trend at mooring 2 (Figure 8) is in good agreement with the observations. The model-predicted water

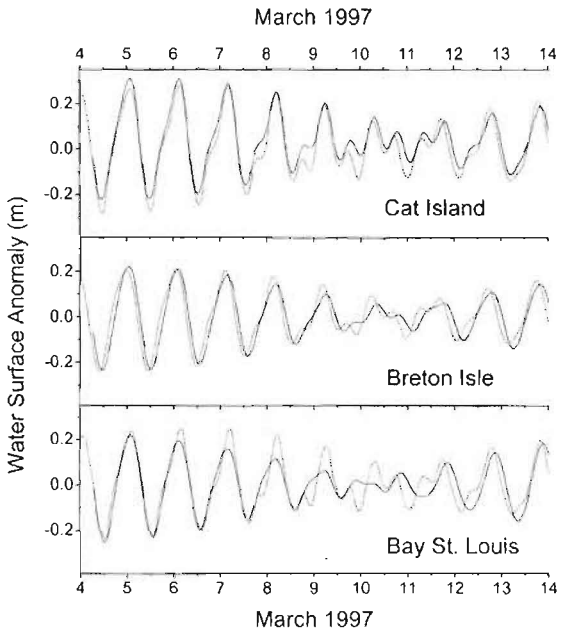

Figure 7. Water surface anomalies predicted from the IHO database (solid line) and predicted by the Princeton Ocean Model (dashed line) at selected stations within the Mississippi bight. The model compared in this figure uses only tidal forcing.

level anomaly is offset by approximately 0.05 to 0.1 m because of the difficulty of removing the mean water depth from the observations. The maximum setdown on March 6 has good amplitude and phase, however. The model predicts a smaller positive water level anomaly (setup) than observed at 0000 GMT on March 7 but it is accurate during the subsequent low tide. Since the tidal elevations at Cat Island (Figure 6) are good, this may be a result of using the winds measured at the NOAA buoy over the entire model domain. Nevertheless, the model demonstrates the correct response sequence, especially during the post-frontal phase when a large setup is accurately predicted.

The model-predicted surface currents at mooring 1 (Figure 9) show the strong tidal flow that is also seen in the measured currents (Figure 5), although the flow is more symmetrical than observed. This is especially true just before the front arrived (after 1200 GMT on March 5). The model does predict a strong perturbation of the tidal flow by the wind on March 7, at which time the southeast currents are stronger than observed. The lack of variability in the modeled currents is probably caused by the use of uniform winds over the entire model domain and the spatial resolution. This is also the likely cause of the over-predicted flow at the end of the simulation.

The waves and currents predicted by the numerical models are in good agreement with the available observations from the Mississippi bight. The ability of the models to predict tidal and wind-driven flows and waves demonstrates their usefulness for examining the physical mechanisms that drive erosion within the region. These comparisons are robust be-

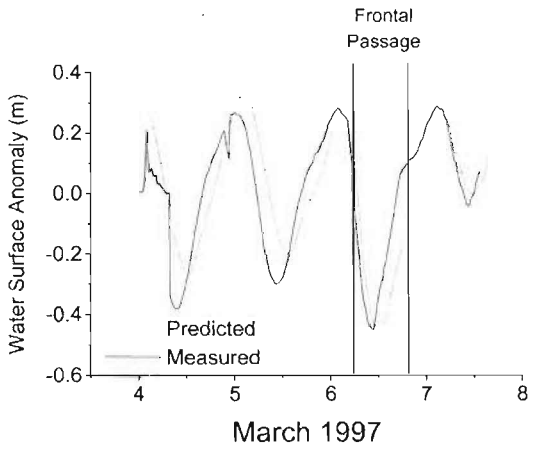

Figure 8. Measured (solid line) and POM-predicted water levels at mooring 2. The model compared in this figure uses both tidal and wind forcing.

cause they were made in complex areas that are good tests of model skill. The modeled waves and currents are less sensitive to uncertainties in forcing and bathymetry within the sounds where waves and currents are more uniform.

Model-Predicted Waves and Currents in the Mississippi Bight

West Ship Island

The largest wave height predicted during frontal passage on March 6 is 0.9 m at the northwest end of WSI (depth = 5 m; see Figure 1 for location), and the maximum wave period is 3.25 s (Figure 10). The wind was westerly at this time. The modeled wave heights and periods decrease for a short time thereafter, because the wind weakened and became west-northwesterly. The predicted surface waves increase again during the post-frontal phase when the wind was north-northwesterly and peak wind speeds occurred. This temporal pattern, which is similar to that observed near Cat Island, is partly caused by the shadowing effect of Cat Island on wave growth during northwesterly winds. The estimated wave steepness remains above 0.04 during the entire cold front, however, suggesting that erosion along the soundside of the island would have occurred whenever the wind had a northerly component.

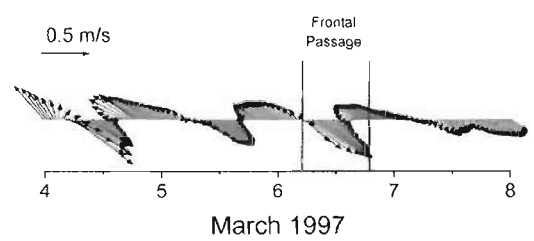

Figure 9. Vector plot of time series of POM-predicted surface currents at mooring 1 with both tides and wind forcing.

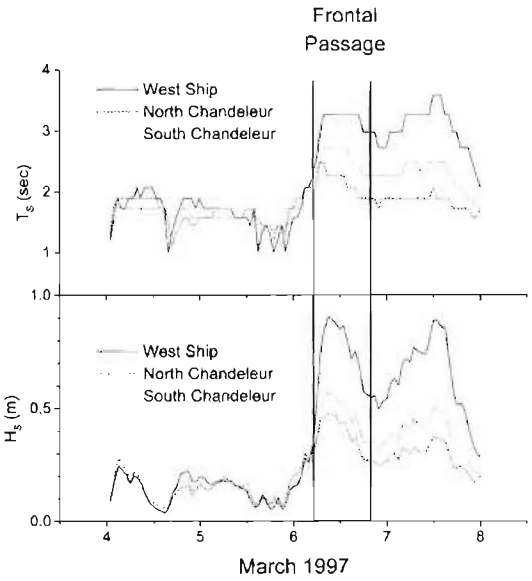

Figure 10. Time series plot of SWAN-predicted significant wave period and height at the locations discussed in the text. See Figure 1 for locations.

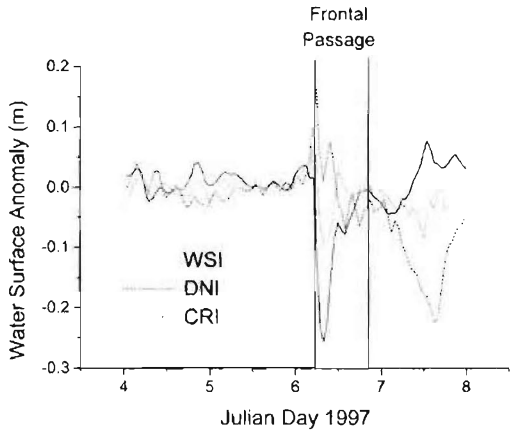

Figure 11. Time series plot of POM-predicted water surface anomalies at selected locations within Mississippi Bight. See Figure 1 for locations.

The mean water level anomalies within the Mississippi bight are calculated using the Princeton Ocean Model with wind forcing only. This simulation indicates the relative magnitude, distribution, and timing of wind-driven setup and setdown within the region. These changes in water level determine which part of the beach face is subjected to wave erosion. The westerly winds during frontal passage pushed water into the eastern end of the sound, producing a predicted setdown of −0.25 m at WSI (Figure 11) and a setup of 0.16 m at Dauphin Island (DNI; see Figure 1 for location). The northerly winds on March 7 produce a predicted setup of 0.07 m on the soundside of WSI and a setdown of −0.22 m at DNI. These results suggest that Dauphin Island is susceptible to setup produced by westerly winds because of restricted exchange between the eastern end of the sound and the Gulf of Mexico.

The current regime within Mississippi Sound is tidally dominated, which is important for wave erosion and transport by steady currents within the sound. The tide was ebbing at 0800 GMT on March 6 when peak waves, generated by westerly winds, are predicted by the SWAN model. The westerly winds would also have reinforced the ebb tide flow, which is generally southeastward. At mid-ebb tide (Figure 12A), the simulated flow rotates southward at WSI and there is a divergence in the velocity field, with surface velocities of 1 m s^{-1} through the inlets. The northerly winds of the post-frontal phase generate larger predicted waves at WSI, which nearly coincide with the low tide on March 7. The hindcast surface currents within the sound (Figure 12B), which are primarily wind-driven at this time because of the low tide, are westward and almost 0.3 m s^{-1} near the western tip of WSI.

Chandeleur Islands

The northern and southern Chandeleur Islands have distinctly different morphologies and responses to forcing. Therefore, this section will discuss waves and currents along the northern segment separately from the southern segment. The predicted waves on the soundside of the northernmost Chandeleur Islands (dashed line in Figure 10) attain a maximum height of 0.48 m during frontal passage in a water depth of 1.5 m. The period reaches a peak of 2.5 s at this time also. The resulting wave steepness parameter is 0.05. The modeled wave height decreases to less than 0.3 m as the wind shifts to westerly, but recovers slightly during the post-frontal phase when the wind is north-northwesterly. Wave-driven southward longshore drift on the soundside of the islands would have persisted throughout the post-frontal phase under the conditions predicted by the model. During the westerly winds accompanying frontal passage, the POM-predicted setup is less than 0.1 m on the soundside of the Chandeleur Islands (dotted line in Figure 11). Driven by the northerly winds of the post-frontal phase, the hindcast steady flow (Figure 13A) bifurcates at the northern tip of the islands, with velocities greater than 1 m s^{-1} on the Gulf side. Although modeled currents are weaker along the western side of the northern islands, they are southward near the coast and would have reinforced wave-driven longshore drift. The POM-predicted steady currents on March 7 (Figure 13b) flow uniformly southward under the northerly winds and longshore flow on the soundside of the northern islands has strengthened slightly. The northerly winds during the post-frontal phase generate a predicted setdown of −0.07 m at the Chandeleurs, which would have reduced beach erosion by waves.

The orientation of the southern Chandeleur Islands makes them more susceptible than the northern Chandeleur Islands to southerly waves from offshore and northwesterly waves generated within Chandeleur Sound. However, shallow water depths within the central part of the sound restrict wave growth during northwesterly winds. Consequently, the hind-

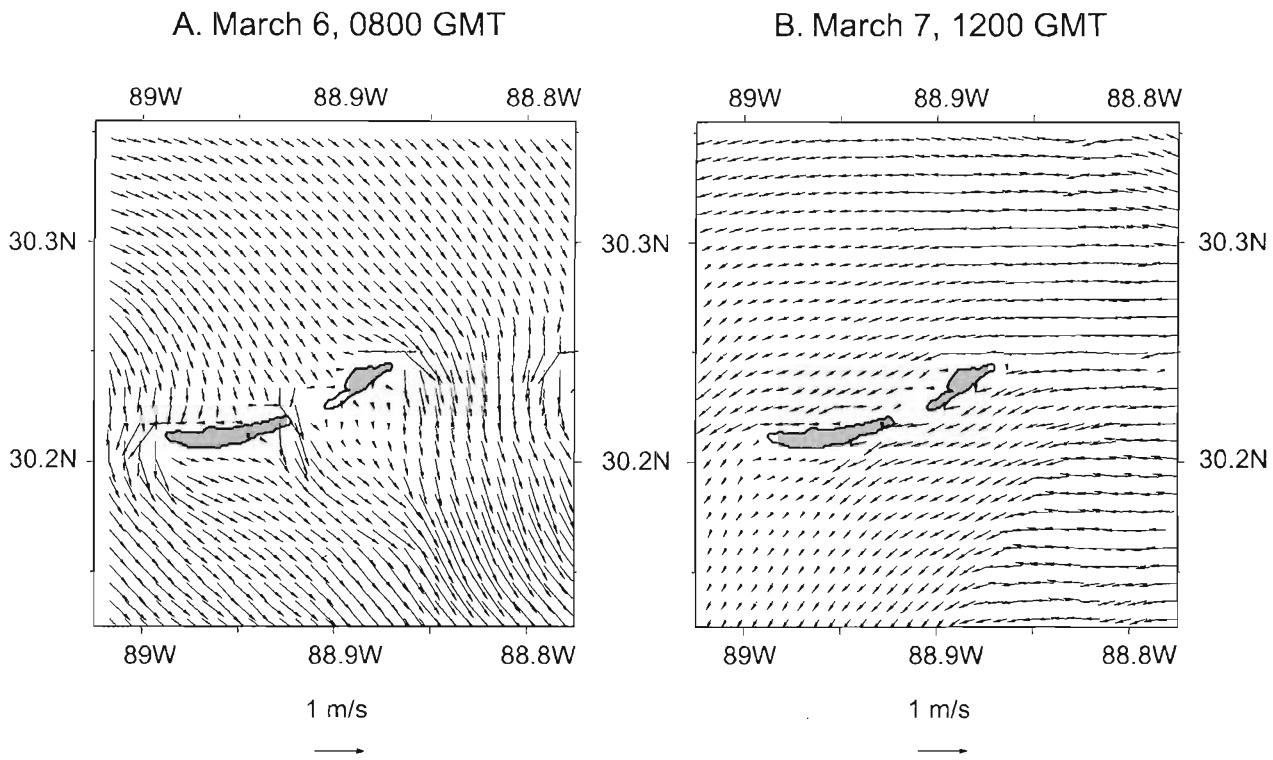

Figure 12. Near-surface currents predicted by the Princeton Ocean Model near West Ship Island. (A) 0800 GMT on March 6. (B) 1200 GMT on March 7. The coastline is for general orientation only and does not exactly match the model grid, which used a higher resolution and newer coastline.

cast significant wave heights and periods (dotted lines in Figure 10) are slightly larger than at the northern end of the islands throughout the cold front. The north-northwesterly winds generate large predicted waves during the post-frontal phase because this is when the wind was strongest. These waves are moderately steep ($H_s/L_0 = 0.04$) and the wave model predicts breaking over the southern Chandeleur shoal. The POM-predicted tidal flow over the shoal is asymmetrical, with ebb currents attaining speeds of more than 1 m s^{-1} on March 6 (Figure 13C), which would have reinforced the ebb tide flow and transported wave-resuspended sediment seaward. The northerly wind during the post-frontal phase on March 7 drives a southward hindcast flow (Figure 13D), which would transport sediment over the shoal into Chandeleur Sound.

DISCUSSION

As suggested by the title of this paper, any discussion of coastal erosion must be somewhat speculative because of the lack of either measurements or model predictions of sediment transport. Nevertheless, it is possible to make several statements because of the robustness of numerical model predictions that have been presented in the previous section.

Implications for Barrier Island Erosion

Erosion along the soundside of the barrier islands is dependent on local water levels, surface waves, and steady currents. This section discusses the contribution of each of these factors to the nearshore environment as it pertains to beach erosion inside the barrier islands. The observations and results from the numerical models indicate how variable these factors can be during a brief meteorological event like a cold front. The sedimentation pattern inferred from the model results should also be robust but the conclusions drawn from it should be consistent with observations of coastal change in the area. Of course, it is expected that the model predictions from this study will also reflect the uniform wind forcing used and that the timing of local maximum waves and wind-driven setup will differ from observations.

Waves can erode the normally subaerial beach whenever the local water level is elevated. Although the setups predicted by the POM (Figure 11) are small, they would raise water levels on the soundside of the islands where there are no protective dunes. Furthermore, these moderate water levels occur frequently and may thus have an important cumulative effect on the long-term evolution of these beaches. Another important factor determining the water level within the sounds is the spring-neap tidal cycle (Figure 7). The tidal amplitude is less than 0.1 m during the neap tide and more than 0.2 m during the spring tide. This combined effect can be seen at Dauphin Island, where a maximum wind-driven setup of 0.16 m is predicted just a few hours after high tide on March 6, but only a few days before the neap tide. Had this occurred during the spring tide, we would expect greater coastal erosion to occur. A second example is seen at Ship Island on March 7, when a

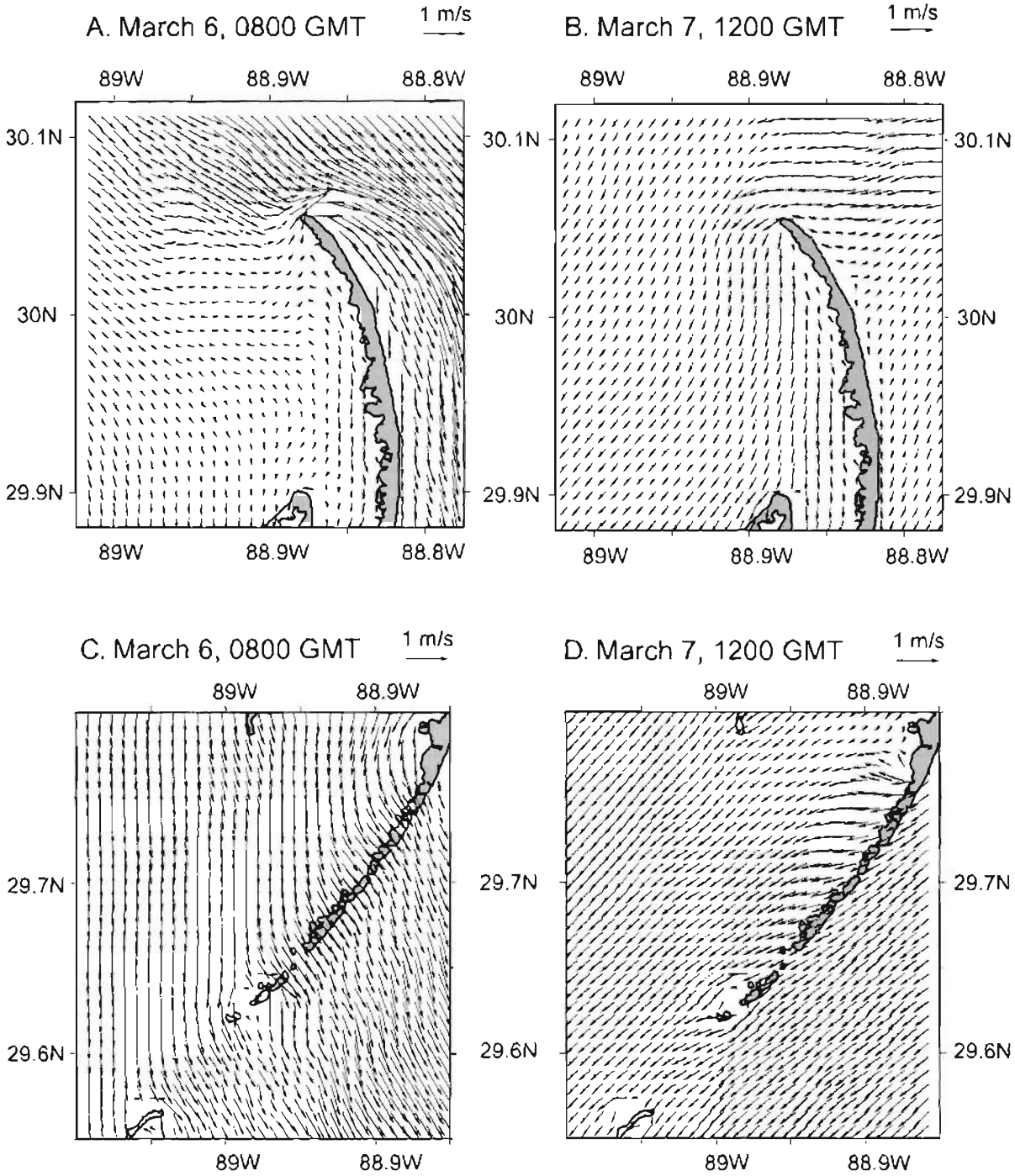

Figure 13. Near-surface currents predicted by the Princeton Ocean Model near the Chandeleur Islands. (A) Near the northern end at 0800 GMT on March 6. (B) Near the northern end at 1200 GMT on March 7. (C) Near the southern end at 0800 GMT on March 6. (D) Near the southern end at 1200 GMT on March 7. The coastline is for general orientation only and does not exactly match the model grid, which used a higher resolution and newer coastline. Note that the southern Chandeleur Islands in C and D are a shoal only in the model.

maximum setup of 0.07 m is predicted during a low tide. Thus, the wind-driven setup and low-tide water levels would have cancelled, and the waves would have been eroding the beach face rather than the berm.

The classical paradigm of coastal erosion predicts that storm waves will transport sediment offshore whereas fair-weather waves, which are less steep, will return sediment to the beach (BRENNINKMEYER, 1978). This model is not entirely

applicable to the beaches within enclosed coastal waters like Mississippi Sound, however. The measured and predicted surface waves during the study interval were steep and would certainly have increased beach erosion. The fair-weather waves within the estuary would not return sand to the beach, however, because there is no long-period swell. Consequently, there will be a cumulative movement of sediment from these beaches to the central parts of the sound. This process would contribute to the observed shoreline retreat of the soundside of the islands (MEYER-ARENDT and GAZZIER, 1990).

Another important process contributing to shoreline retreat is wave-driven longshore transport, which is the dominant fair-weather sediment transport process on open ocean beaches in the northern Gulf of Mexico (STONE and STAPOR, 1996). However, the lack of long-period, swell-like waves within the sound precludes the generation of large littoral cells within the sound. Instead, longshore drift should be weak and short-lived, responding rapidly to changes in wind and wave direction. The surface waves were steepest during westerly and northerly winds. Thus, it is reasonable to conclude that longshore drift on the soundside of the northern islands was eastward during frontal passage. However, as the wind became northeasterly during the post-frontal phase, longshore drift would have reversed direction.

Sediment transport by downwelling mean currents is the dominant mechanism for across-shore transport on the shoreface of open ocean beaches during storms (WRIGHT *et al.*, 1991). Across-shore transport was probably not very efficient within the sounds during most of the cold front because of the shallow water depths and well-mixed water column. The mean currents predicted by the POM indicate that sediment transport during frontal passage would have been westward on the shoreface at WSI (Figure 12A), in opposition to wave-driven longshore drift in the surf zone, and eastward at ESI. Current-driven shoreface transport would have been westward at Ship Island after the wind shifted to more northerly during the post-frontal phase (Figure 12B). Divergence and convergence of alongshore transport causes local erosion and deposition, respectively (KEELEY, 1977; SÁNCHEZ-ARCILLA *et al.*, 2001). Consequently, the steady currents in Figure 12 suggest that sediment would have been continuously eroded from WSI and transported into Ship Island Pass to the west. Such a transport system during cold fronts partly explains the long-term erosion at the western end of Ship Island (STONE *et al.*, 1998).

The extensive mean southward flow on the soundside of the Chandeleur Islands (Figure 13) would have supplemented sediment transport within the littoral sedimentation cell generated by the wave field. This combined transport would have supplied sediment to the southern Chandeleur Islands (actually a shoal) for all wind conditions during the cold front. During the westerly winds on March 6, sediment delivered to the shoal would have been transported seaward and deposited on the Gulf side where the flow decelerates. Northerly winds would have produced an even stronger southward transport on the Gulf side of the shoal. This sedimentation pattern suggests that northwestward migration of the islands by overwash during tropical cyclones is opposed by southwest and southeast migration during cold fronts. This cold-front sedimentation pattern would contribute to the rapid recovery of the islands after hurricanes (KAHN and ROBERTS, 1982). Southward longshore transport on the Gulf side during the cold front is also in opposition to northward wave-driven drift during fairweather conditions (PENLAND and SUTER, 1988).

Predicting Coastal Change

General principles of sedimentation have allowed patterns of erosion and sediment transport to be inferred from the model-predicted waves and currents presented in this paper. These estimates are necessarily qualitative and lacking in detail because no sediment entrainment and transport calculations were completed. In order to make quantitative predictions of coastline change during the cold front, it is necessary to couple the wave and current results to a nearshore sedimentation model. This coupling can be accomplished by embedding a three-dimensional numerical sedimentation model within a hydrodynamic model (*e.g.*, ZEIGLER and NISBET, 1994; SIGNELL and HARRIS, 2000; SCHEFFNER, 2000) or driving a stand-alone sedimentation model with either observations or model output (*e.g.*, KEEN and STAVN, 2000; JONES and LICK, 2000). Alternatively, model-predicted waves and currents could be used as input for other kinds of coastal sedimentation models. For example, high-resolution simulated waves can be applied to process-response models (*e.g.*, WRIGHT and SHORT, 1984), thereby permitting detailed spatial analyses of coastline change. Similarly, mathematical models (*e.g.*, FOX and DAVIS, 1973; HANSON and KRAUS, 1989) can be used when observations of waves and currents are not available, thus improving both short- and long-term forecasting. The most rigorous use of numerical wave and current models is to drive numerical sedimentation models, which can take advantage of their good spatial coverage and temporal output (*e.g.*, RAKHA, 1998).

SUMMARY

This study applies numerical wave and current models to understanding the forcing that determined barrier island erosion during a winter cold front that passed over the Mississippi bight in the Gulf of Mexico on March 6, 1997. The SWAN wave model was used to predict waves, and the Princeton Ocean Model was used to hindcast water levels and steady currents. The model predictions are in good agreement with available observations.

The hindcast waves within Mississippi Sound reach heights of 0.9 m during the cold front. The wave periods within the enclosed sounds do not exceed 3.5 s and, consequently, the wave steepness parameter, H_S/L_0, remains above 0.4 throughout the cold front. Littoral transport would have been predominantly eastward until the wind became northeasterly, at which time it would have reversed direction. Currents within Mississippi Sound are dominated by tidal flow during the cold front, and sediment transport on the shoreface is thus sensitive to the tidal stage.

Hindcast waves along the soundside of the Chandeleur Islands (north-south trending) range from 0.45 m in the north to 0.55 m in the south. The tidal currents in Chandeleur

Sound are less variable than in Mississippi Sound and it appears that sediment transport would have been continuously southward throughout the island chain because of the combination of wave-driven longshore drift in the surf zone and steady currents on the shore face. Occasional spillover onto the Gulf side of the islands is predicted during the frontal passage phase when the wind was westerly.

The inferred erosion and sediment transport patterns based on the model results are consistent with observations of long-term shoreline change in Mississippi Sound, as well as sedimentation processes that control shoreline change in the Chandeleur Island chain. The waves and currents that can be simulated with modern numerical models are well suited to drive all types of coastal sedimentation and geomorphic models. The problem of getting good numerical hindcasts and forecasts has decreased in recent years as coastal observing and forecasting systems are being developed. Thus, the coastal researcher is no longer restricted to available observations and historical databases. This has exciting consequences for studying coastal change in the near future.

ACKNOWLEDGMENTS

The Office of Naval Research, program element 62435N, sponsored this work. Modeling requirements in support of the Northern Gulf of Mexico Littoral Initiative project of the Naval Oceanographic Office motivated this study. The author also thanks Erick Rogers for advice on the use and interpretation of the SWAN wave model.

LITERATURE CITED

ADDAD, J. and MARTINS-NETO, M.A., 2000. Deforestation and coastal erosion: A case study from Brazil. *Journal of Coastal Research,* 16 (2), 423–431.

AHSAN, Q.; BARRON, C.N.; BLAHA, J.; BLUMBERG, A.F.; FITZPATRICK, P.J.; HERNDON, D.; HERRING, H.J.; HSU, Y.L.; KEEN, T.R.; LI, H.; LI, Y.; PATCHEN, R.C.; SZCZECHOWSKI, C.; WILLEMS, R., and WILZ, P., 2001. Northern Gulf of Mexico Littoral Initiative Modeling Program. *Proceedings, 7th Estuarine and Coastal Modeling Conference.* New York: American Society of Civil Engineers, submitted.

AIKMAN, F.; MELLOR, G.L.; EZER, T.; SHEININ, D.; CHEN, P.; BREAKER, L.; BOSLEY, K., and RAO, D.B., 1996. Towards an operational nowcast/forecast system for the U.S. East Coast. *In:* MALANOTTE-RIZZOLI, P. (ed.), *Modern Approaches to Data Assimilation in Ocean Modeling, Elsevier Oceanographic Series 61.* New York: Elsevier, pp. 347–376.

BAILLARD, J.A., 1982. Modeling on-offshore sediment transport in the surf zone. *Proceedings, 18th Coastal Engineering Conference.* New York: American Society of Civil Engineers, pp. 1419–1438.

BLUMBERG, A.F.; AHSAN, Q., and LEWIS, J.K., 2000. Modeling hydrodynamics of the Mississippi Sound and adjoining rivers, bays and shelf waters. *Oceans 2000 Conference Proceedings.* Marine Technology Society.

BOOIJ, N.; RIS, R.C., and HOLTHUIJSEN, L. H., 1999. A third generation wave model for coastal regions: 1. Model description and validation. *Journal of Geophysical Research,* 104, 7649–7666.

BOWEN, A.J., 1980. Simple models of nearshore sedimentation: Beach profiles and longshore bars. *In:* MCCANN, S.B. (ed.), *The Coastline of Canada. Geological Survey of Canada Paper No. 80–10,* pp. 1–11.

BRENNINKMEYER, B.M., 1978. Littoral sedimentation. *In:* FAIRBRIDGE, S.B. and BOURGEOIS, J. (eds.), *The Encyclopedia of Sedimentology.* Stroudsburg, Pennsylvania: Dowden, Hutchinson and Ross, pp. 448–457.

BRUUN, P., 1954. Coast erosion and the development of beach profiles. Beach Erosion Board Technical Memoir No. 44. U.S. Army Corps of Engineers.

CHANEY, P.L. and STONE, G.W., 1996. Soundside erosion of a nourished beach and implications for winter cold front forcing: West Ship Island, Mississippi. *Shore and Beach,* 64, 27–33.

CIPRIANI, L.E. and STONE, G.W., 2001. Net longshore sediment transport and textural changes in beach sediments along the southwest Alabama and Mississippi barrier islands, U.S.A. *Journal of Coastal Research,* 17 (2), 443–458.

CLANCY, R.M.; DEWITT, P.W.; MAY, P., and KO, D.S., 1996. Implementation of a coastal ocean circulation model for the west coast of the United States. *Proceedings of the American Meteorological Society Conference on Oceanic and Atmospheric Prediction.* pp. 72–75.

DALLY, W.R. and DEAN, R.G., 1984. Suspended sediment transport and beach profile evolution. *Journal of Waterway, Port, Coastal and Ocean Engineering,* 110, 15–33.

DAVIS, R.A., JR. and FOX, W.T., 1975. Process-response patterns in beach and nearshore sedimentation: 1. Mustang Island, Texas. *Journal of Sedimentary Petrology,* 45 (4), 852–865.

DINGLER, J.R.; REISS, T.E., and PLANT, N.G., 1993. Erosional patterns of the Isles Derniers, Louisiana, in relation to meteorological influences. *Journal of Coastal Research,* 9 (1), 112–125.

DOLAN, R.; LINS, H., and HAYDEN, B., 1988. Mid-Atlantic coastal storms. *Journal of Coastal Research,* 4 (3), 417–433.

FENSTER, M. and DOLAN, R., 1994. Large-scale reversals in shoreline trends along the United States mid-Atlantic coast. *Geology,* 22 (6), 543–546.

FLATHER, R.A., 1976. A tidal model of the north-west European continental shelf. *Memoirs of the Royal Science Society of Liège,* 10, 141–164.

FOX, W.T. and DAVIS, R.A., JR., 1973. Simulation model for storm cycles and beach erosion on Lake Michigan. *Geological Society of America Bulletin,* 84, 1769–1790.

FRIEDMAN, G.M. and SANDERS, J.E., 1978. *Principles of Sedimentology.* New York: John Wiley and Sons, 792 pp.

HANSON, H. and KRAUS, N.C., 1989. Genesis: Generalized Model for Simulating Shoreline Change. Technical Report CERC-89-19, Coastal Engineering Research Center, U.S. Army Corps of Engineers, Waterways Experiment Station, Vicksburg, Mississippi.

HARDING, J.; CARNES, M.C.; PRELLER, R.H., and RHODES, R., 1999. The Naval Research Laboratory's role in naval ocean prediction. *Marine Technology Society Journal,* 33, 67–79.

HASSELMANN, K.; BARNETT, T.P.; BOUWS, E.; CARLSON, H.; CARTWRIGHT, D.E.; ENKE, K.; EWING, J.A.; GIENAPP, H.; HASSELMANN, D.E.; KRUSEMAN, P.; MEERBURG, A.; MULLER, P.; OLBERS, D.J.; RICHTER, K.; WELL, W., and WALDEN, H., 1973. Measurements of wind-wave growth and swell decay during the Joint North Sea Wave Project (JONSWAP). *Deutsch Hydrographie Zeitschrift,* Supplement, 12, A8.

HAYDEN, B.P., 1999. Climate change and extratropical storminess: An assessment. *Journal of the American Water Resources Association,* 35 (6), 1387–1397.

HORTON, C.; CLIFFORD, M.; COLE, D.; SCHMITZ, J., and KANTHA, L., 1992. Operational modeling: semi-enclosed basin modeling at the Naval Oceanographic Office. *Oceanography,* 5, 69–72.

HSU, Y.L.; ROGERS, W.E.; KAIHATU, J.M., and ALLARD, R.A., 2000. Application of SWAN in the Mississippi Sound. *Proceedings of the Sixth International Workshop on Wave Hindcasting and Forecasting, Monterey, California.* Meteorological Service of Canada, 398–403.

HUH, O.K.; WALKER, N.D., and MOELLER, C., 2001. Sedimentation along the eastern Chenier Plain coast: Down drift impact of a delta complex shift. *Journal of Coastal Research,* 17 (1), 72–81.

JONES, G., 1994. Global warming, sea-level change and the impact on estuaries. *Marine Pollution Bulletin,* 28 (1), 7–14.

JONES, C. and LICK, W., 2000. Effects of bed coarsening on sediment transport. *Proceedings, 6th Estuarine and Coastal Modeling Con-*

ference. New York: American Society of Civil Engineers, pp. 915–930.

KAHN, J.H. and ROBERTS, H.H., 1982. Variations in storm response along a microtidal transgressive barrier-island arc. *Sedimentary Geology,* 33, 129–146.

KEELEY, J. R., 1977. Nearshore currents and beach topography, Martinique Beach, Nova Scotia, *Canadian Journal of Earth Sciences,* 14, 1906–1915.

KEEN, T.R. and SLINGERLAND, R.L., 1993. A numerical study of sediment transport and event bed genesis during Tropical Storm Delia. *Journal of Geophysical Research,* 98, 4775–4791.

KEEN, T.R. and STAVN, R.H., 2000. Developing a capability to forecast coastal ocean optics: Minerogenic scattering. *Proceedings, 6th Estuarine and Coastal Modeling Conference.* New York: American Society of Civil Engineers, pp. 178–193.

KIM, S.C.; WRIGHT, L.D.; MAA, J.P.Y., and SHEN, J., 1998. Morphodynamic responses to extratropical meteorological forcing on the inner shelf of the Middle Atlantic Bight: wind waves, currents, and suspended sediment transport. *Proceedings, 5th Estuarine and Coastal Modeling Conference.* New York: American Society of Civil Engineers, pp. 456–466.

KNOWLES, S.C. and ROSATI, J., 1988. Gulfport Harbor, Mississippi: General design memorandum No. 1, appendix B, hydrodynamics. U.S. Army Corps of Engineers, Mobile District, 76 pp.

LAWRENCE, M.B.; MAYFIELD, B.M.; AVILA, L.A.; PASCH, R.J., and RAPPAPORT, E.N., 1998. Atlantic hurricane season of 1995. *Monthly Weather Review,* 126 (5), 1124–1151.

LEHFELDT, R. and BARTHEL, V., 2000. MORWIN—Collaborative modeling of coastal morphodynamics. *Proceedings, 6th Estuarine and Coastal Modeling Conference,* New York: American Society of Civil Engineers, pp. 1192–1205.

LEUTTICH, R.A.; WESTERINK, J.J., and SCHEFFNER, N.W., 1992. ADCIRC: An advanced three-dimensional circulation model for shelves, coasts, and estuaries. Report 1: Theory and methodology of ADCIRC-2DDI and ADCIRC-3DI. Technical Report DRP-92-6. Department of the Army, 168 pp.

MELLOR, G.L. and YAMADA, T., 1982. Development of a turbulence-closure model for geophysical fluid problems. *Review of Geophysics,* 20, 851–875.

MEYER-ARENDT, K.J. and GAZZIER, C.A., 1990. Shoreline erosion and wetland loss in Mississippi. *Transactions of the Gulf Coast Association of Geological Societies,* 50, 599.

MOELLER, C.C.; HUH, O.K.; ROBERTS, H.H.; GUMLEY, L.E., and MENZEL, W.P., 1993. Response of Louisiana Coastal Environments to a cold front passage. *Journal of Coastal Research,* 9 (2), 434–447.

NUMMEDAL, D.; PENLAND, S.; GERDES, R.; SCHRAMM, W.; KAHN, J., and ROBERTS, H., 1980. Geologic response to hurricane impact on low-profile Gulf Coast barriers. *Transactions of the Gulf Coast Association of Geological Societies,* 30, 183–195.

OEY, L. and CHEN, P., 1992. A nested grid ocean model: With application to the simulation of meanders and eddies in the Norwegian coastal current. *Journal of Geophysical Research,* 97, 20063–20086.

OTVOS, E.G., 1970. Development and migration of barrier islands, northern Gulf of Mexico. *Geological Society of America Bulletin,* 81, 241–246.

OTVOS, E.G., 1979. Barrier island evolution and history of migration, north central Gulf coast. *In:* LEATHERMAN, S.P. (ed.), *Barrier Islands from the Gulf of St. Lawrence to the Gulf of Mexico,* 291–319.

PENLAND, S. and SUTER, J.R., 1988. Barrier island erosion and protection in Louisiana: A coastal geomorphological perspective. *Transactions of the Gulf Coast Association of Geological Societies,* 38, 331–342.

PEREZ, B.C.; DAY, J.W.; ROUSE, L.J.; SHAW, R.F., and WANG, R., 2000. Influence of Atchafalaya River discharge and winter frontal passage on suspended sediment concentration and flux in Fourleague Bay, Louisiana. *Estuarine Coastal and Shelf Science,* 50 (2), 271–290.

PIELKE, R.A. and LANDSEA, C.W., 1998. Normalized hurricane damage in the United States: 1925–95. *Weather and Forecasting,* 13 (3), 621–631.

RAKHA, K.A., 1998. A quasi-3D phase-resolving hydrodynamic and sediment transport model. *Coastal Engineering,* 34, 277–311.

RIS, R.C.; HOLTHUIJSEN, L.H., and BOOIJ, N., 1999. A third generation wave model for coastal regions: 2. Verification. *Journal of Geophysical Research,* 104, 7667–7681.

ROBERTS, H.H.; HUH, O.K.; HSU, S.A.; ROUSE, L.J., JR., and RICKMAN, D., 1987. Impact of cold-front passages on geomorphic evolution and sediment dynamics of the complex Louisiana coast. *Coastal Sediments '87, Proceedings of a Specialty Conference* (May 12–14, 1987, New Orleans, Louisiana). New York: American Society of Civil Engineers, pp. 1950–1963.

ROGERS, W.E.; HWANG, P.A., and WANG, D.W., 2001. Investigation of wave growth and decay in a wave action model. *Journal of Physical Oceanography,* Submitted.

RUCKER, J.B. and SNOWDEN, J.O., 1990. Barrier island evolution and reworking by inlet migration along the Mississippi-Alabama Gulf coast. *Transactions of the Gulf Coast Association of Geological Societies,* 40, 745–753.

SÁNCHEZ-ARCILLA, A.; JIMÉNEZ, J. A.; VALDEMORO, H. I.; GRACIA, V., and GALOFRÉ, J., 2001. Sensitivity analysis of longshore sediment transport rate estimations in a highly eroding coast, the Montroig Beach (Tarragona, Spain). *Coastal Dynamics '01,* pp. 112–121.

SCHEFFNER, N.W., 2000. A large domain convection diffusion based finite element transport model. *Proceedings, 6th Estuarine and Coastal Modeling Conference.* New York: American Society of Civil Engineers, pp. 194–208.

SCHMALZ, R.A., 2000. Development of a nowcast/forecast system for Galveston Bay. *Proceedings, 6th Estuarine and Coastal Modeling Conference.* New York: American Society of Civil Engineers, pp. 441–455.

SCHWAB, D.J. and BEDFORD, K.W., 1994. Initial implementation of the Great Lakes Forecasting System: a real-time system for predicting lake circulation and thermal structure. *Water Pollution Research Journal of Canada,* 29, 203–220.

SIGNELL, R. P. and HARRIS, C. K., 2000. Modeling sand bank formation around tidal headlands. *Proceedings, 6th Estuarine and Coastal Modeling Conference.* New York: American Society of Civil Engineers, pp. 209–222.

STONE, G.W. and FINKL, C.W. (eds.), 1995. Impacts of Hurricane Andrew on the coastal zones of Louisiana and Florida; August 22–26, 1992. *Journal of Coastal Research Special Issue* 21.

STONE, G.W. and STAPOR, F.W., 1996. A nearshore sediment transport model for the northeast Gulf of Mexico coast. *Journal of Coastal Research,* 12 (3), 786–792.

STONE, G.W. and WANG, P., 1999. The importance of cyclogenesis on the short-term evolution of Gulf coast barriers. *Transactions of the Gulf Coast Association of Geological Societies,* 49, 47–48.

STONE, G.W.; GRYMES; J.W.; DINGLER, J.R., and PEPPER, D.A., 1997. Overview and significance of hurricanes on the Louisiana Coast, U.S.A. *Journal of Coastal Research,* 134 (3), 656–669.

STONE, G.W.; CHANEY, P.; WANG, P., and ZHANG, X., 1998. Beach nourishment monitoring program at Fort Massachusetts, West Ship Island, Mississippi, Volumes 1–4. Report to National Park Service. Baton Rouge, Louisiana: Coastal Studies Institute, Louisiana State University.

SUTER, J.R.; PENLAND, S.; WILLIAMS, S.J., and KINDINGER, J.L., 1988. Transgressive evolution of the Chandeleur Islands, Louisiana. *Transactions of the Gulf Coast Association of Geological Societies, 38, 315–322.*

THIELER, E.R.; PILKEY, O.H.; YOUNG, R.S.; BUSH, D.M., and CHAI, F., 2000. The use of mathematical models to predict beach behavior for U.S. coastal engineering: A critical review. *Journal of Coastal Research,* 16, 48–70.

UPSHAW, C.F.; CREATH, W.B., and BROOKS, F.L., 1966. Sediments and microfauna off the coasts of Mississippi and adjacent states. *Mississippi Geological Survey Bulletin,* 106, 127 pp.

VINCENT, M.; BURWELL, D., and LUTHER, M., 2000. The Tampa Bay nowcast-forecast system. *Proceedings, 6th Estuarine and Coastal Modeling Conference.* New York: American Society of Civil Engineers, pp. 765–780.

WAMDI Group, 1988. The WAM model: A third generation ocean

wave prediction model. *Journal of Physical Oceanography,* 18, 1775–1810.

WRIGHT, L.D. and SHORT, A.D., 1984. Morphodynamic variability of surf zones and beaches: A synthesis. *Marine Geology,* 26, 93–118.

WRIGHT, L.D.; BOON, J.D.; KIM, S.C., and LIST, J.H., 1991. Modes of cross-shore sediment transport on the shoreface of the Middle Atlantic Bight. *Marine Geology,* 19–51.

YOUNG, D.R.; SHAO, G.F., and BRINSON, M.M., 1995. The impact of the October 1991 northeaster storm on barrier-island shrub thickets (*Myrica-cerifera*). *Journal of Coastal Research,* 11 (4), 1322–1328.

ZEIGLER, C.K. and NISBET, B.S., 1994. Fine-grained sediment transport in Pawtuxet River, Rhode Island. *Journal of Hydraulic Engineering,* 120 (5), 561–576.

ZHANG, K.Q.; DOUGLAS, B.C., and LEATHERMAN, S.P., 2000. Twentieth-century storm activity along the U.S. east coast. *Journal of Climate,* 13 (10), 1748–1761.